applied sciences

MDPI

Article

Isatin-Hydrazones with Multiple Receptor Tyrosine Kinases (RTKs) Inhibitory Activity and In-Silico Binding Mechanism

Huda S. Al-Salem [1,*], Md Arifuzzaman [2], Iman S. Issa [1] and A. F. M. Motiur Rahman [1,*]

[1] Department of Pharmaceutical Chemistry, College of Pharmacy, King Saud University, Riyadh 11451, Saudi Arabia; iman_issa69@yahoo.com
[2] College of Pharmacy, Yeungnam University, Gyeongsan 38541, Korea; arifmilon2016@ynu.ac.kr
* Correspondence: hhalsalem@ksu.edu.sa (H.S.A.-S.); afmrahman@ksu.edu.sa (A.F.M.M.R.); Tel.: +966-11-29-52740 (H.S.A.-S.); +966-11-46-70237 (A.F.M.M.R.)

Abstract: Recently, we have reported a series of isatin hydrazone, two of them, namely, 3-((2,6-dichlorobenzylidene)hydrazono)indolin-2-one (**1**) and 3-((2-chloro-6-fluorobenzylidene)hydrazono) indolin-2-one (**2**) having potent cytotoxicity, showing cyclin-dependent kinases (CDK2) inhibitory activity and bearing recommended drug likeness properties. Since both compounds (**1** and **2**) showed inhibitory activity against CDK2, we assumed it would also have multiple receptor tyrosine kinases (RTKs) inhibitory activity. Considering those points, here, above-mentioned two isatin hydrazone **1** and **2** were synthesized using previously reported method for further investigation of their potency on RTKs (EGFR, VEGFR-2 and FLT-3) inhibitory activity. As expected, Compound **1** exhibited excellent inhibitory activity against epidermal growth factor receptor (EGFR, IC_{50} = 0.269 μM), vascular epidermal growth factor receptor 2 (VEGFR-2, IC_{50} = 0.232 μM) and FMS-like tyrosine kinase-3 (FLT-3, IC_{50} = 1.535 μM) tyrosine kinases. On the other hand, Compound **2** also exhibited excellent inhibitory activity against EGFR (IC_{50} = 0.369 μM), VEGFR-2 (IC_{50} = 0.266 μM) and FLT-3 (IC_{50} = 0.546 μM) tyrosine kinases. A molecular docking study with EGFR, VEGFR-2 and FLT-3 kinase suggested that both compounds act as type I ATP competitive inhibitors against EGFR and VEGFR-2, and type II ATP non-competitive inhibitors against FLT-3.

Keywords: isatin-hydrazones; EGFR inhibitor; VEGFR-2 inhibitor; FLT-3 inhibitor

check for updates

Citation: Al-Salem, H.S.; Arifuzzaman, M.; Issa, I.S.; Rahman, A.F.M.M. Isatin-Hydrazones with Multiple Receptor Tyrosine Kinases (RTKs) Inhibitory Activity and In-Silico Binding Mechanism. *Appl. Sci.* **2021**, *11*, 3746. https://doi.org/10.3390/app11093746

Academic Editor: Mariusz Mojzych

Received: 31 March 2021
Accepted: 19 April 2021
Published: 21 April 2021

1. Introduction

Cancer is not only a complex disease but it also life threatening [1]. Therefore, development of an excellent anticancer agents are very much essential, especially ones with potent biological activities, enzyme inhibitory activities and low/no toxicity [2–5] (Figure 1). Regarding enzyme inhibitory activities: (i) cyclin-dependent kinases (CDKs) are considered as a vital feature, inciting various key transitions in the cell cycle for cancer cells, in addition to instructing apoptosis, transcription and exocytosis; (ii) the epidermal growth factor receptor (EGFR) [6] kinase enzyme promote overexpression, and overexpression of certain proteins may play a role in various cancer development [7–15]; (iii) the vascular endothelial growth factor receptor 2 (VEGFR-2) [16,17] is highly expressed in tumor-associated endothelial cells, where it modulates tumor-promoting angiogenesis, and it is also found on the surface of tumor cells [18]; (iv) FMS-like tyrosine kinase-3 (FLT-3) is a protein found in humans and is encoded by the FLT-3 gene [19–21]. Mutations of the FLT-3 receptor can lead to the development of leukemia, a cancer of bone marrow hematopoietic progenitors [22–25]. The development of a cancer may be delayed or cured by inhibition of those kinase enzymes. Recently, a number of researches have been focusing on how to block EGFR kinase enzyme activity, applying synthetic organic molecules [26] such as imatinib [27], which is used in treating gastrointestinal stromal tumors (GISTs), chronic myelogenous leukemia (CML) and malignancies. Erlotinib [28], is used in the treatment of pancreatic cancer, non-small cell

lung cancer (NSCLC) and several other types of cancer, but the mechanism of clinical antitumor action of erlotinib is not fully characterized. Neratinib [29–31], is exhibits antitumor action against EGFR, HER2, and HER4 positive carcinomas and used as an extended adjuvant treatment in adult patients with early stage HER2-overexpressed/amplified breast cancer, to follow adjuvant trastuzumab-based therapy. Sorafenib [32], is indicated for the treatment of unrespectable hepatocellular carcinoma and advanced renal cell carcinoma. Crizotinib [33–35], is used for the treatment of locally advanced or metastatic NSCLC that is anaplastic-lymphoma kinase (ALK)-positive as detected by a FDA-approved test. Further, many others [36–41] inhibit VEGFR-2 kinase [42–51] and FLT-3 kinase enzyme activities [25,52–57]. However, most of them reported adverse reactions, which were edema, nausea, vomiting, muscle cramps, rash, diarrhea, fatigue and abdominal pain, etc. In our previous report [5], we have highlighted CDK2 kinase inhibitors (**1** and **2**), which act as potential type-II ATP competitive inhibitor, have two-fold cytotoxicity for Compound **1** (IC_{50} = 1.51 μM) and have similar cytotoxicity for Compound **2** (IC_{50} = 3.56 μM) comparing with known anticancer drug doxorubicin (IC_{50} = 3.1 μM) against human breast adenocarcinoma (MCF7) with recommended drug likeness properties. Those reported results for Compounds **1** and **2** motivated us to do further inhibitory activities against EGFR, VEGFR-2 and FLT-3 protein kinase enzymes with their docking simulations in order to explore the behavior of **1** and **2** within the active site of EGFR, VEGFR-2 and FLT-3 to justify its binding mechanism.

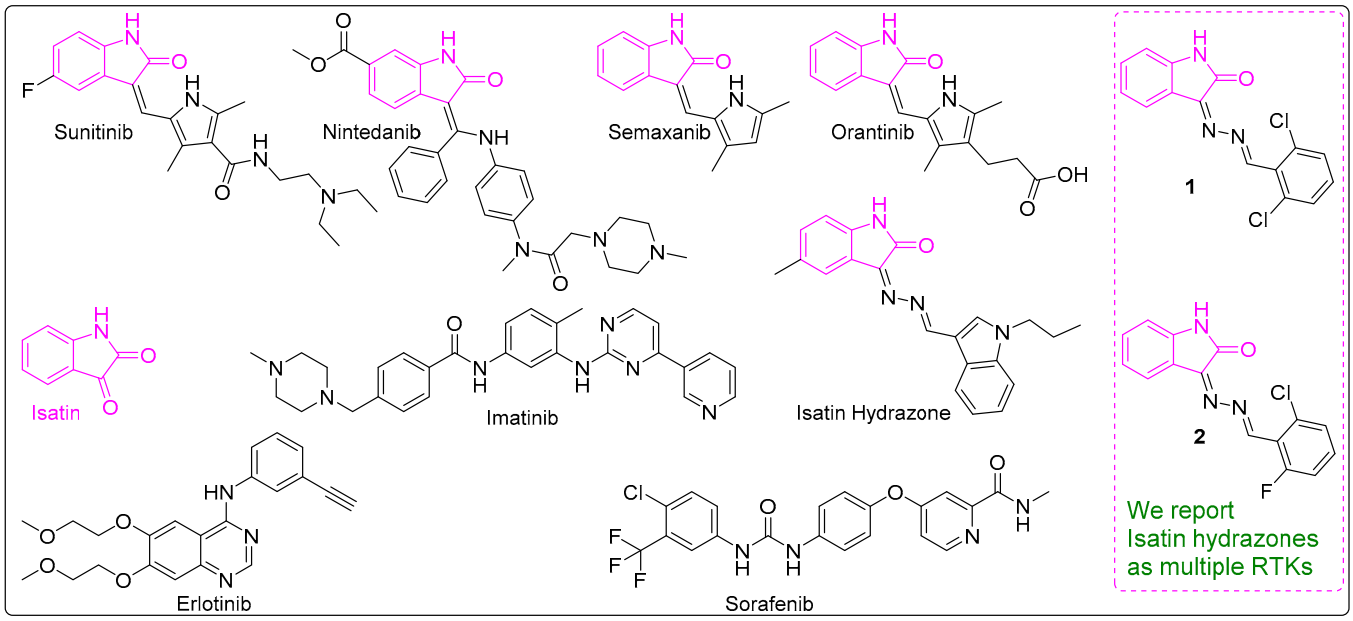

Figure 1. Structure of isatin, some RTKs inhibitors, and Compounds **1** and **2** having isatin skeleton.

2. Materials and Methods

2.1. General

Solvents and chemicals were reagent grade (Sigma-Aldrich, St. Louis, MO, USA) and were used without further purification. Electrothermal IA9100 (Stone, Stafforshire, ST15 OSA, UK) equipment were used to measure the melting points of synthesized product. IR spectra were taken on a Perkin Elmer FT-IR Spectrum BX device (Ayer Rajah Crescent, Singapore). The 600 MHz Bruker NMR spectrometer (Reinstetten, Germany) was used for taking NMR (1H & 13C) spectra. An Agilent 6410 QQQ mass spectrometer was used to take mass of the synthesized compounds (Agilent Technologies, Palo Alto, CA, USA).

2.2. General Procedure for the Synthesis of Isatin-Hydrazones

A mixture of 3-hydrazineylideneindolin-2-one (5 mmol) and 2,6-dichlorobenzyldehyde/2-chloro-6-fluorobenzaldehyde (5 mmol) in absolute ethanol (15 mL), and a few drops of glacial acetic acid were added. The reaction mixture was refluxed for 4 h. The completion of the reaction was monitored by TLC. The precipitate solid was filtered, washed with cold ethanol, air dried, and further recrystallized from ethanol to give pure 3-((2,6-dichlorobenzylidene)hydrazono)indolin-2-one (**1**)/3-((2-chloro-6-fluorobenzylidene)hydrazono)indolin-2-one (**2**). **1**: Orange powder (98%). m.p. = 286–287 °C (m.p. = 286–287 °C [5]); **2**: Reddish brown solid (75%). m.p. = 277–778 °C (m.p. = 277–778 °C [5]).

2.3. Calculation of the IC_{50} Values

Calculation of the IC_{50} values of EGFR, VEGFR-2 and FLT-3 inhibitory assays was performed using linear equation (y = mx + c) for log concentration vs. percentage of inhibition, and detailed results were inserted in the supporting material.

2.4. In Vitro EGFR/VEGFR-2 Inhibitory Activity

The EGFR/VEGFR-2 assay kit was designed to measure EGFR/VEGFR-2 inhibitory activity for screening and profiling applications, using Kinase-Glo® MAX as a detection reagent. The EGFR/VEGFR-2 assay kit comes in a convenient 96-well format, with enough purified recombinant EGFR/VEGFR-2 enzyme, EGFR/VEGFR-2 substrate, ATP and kinase buffer 1 for 100 enzyme reactions. The assay was performed according to the protocol supplied from the EGFR/VEGFR-2 kinase assay kit #40321 (BPS Bioscience, San Diego, CA, USA) and #40325 (BPS Bioscience, San Diego, CA, USA), respectively [58,59]. The EGFR/VEGFR-2 activity at a single dose concentration of 10 μM was performed, where the Kinase-Glo MAX luminescence kinase assay kit (Promega#V6071) was used. The compounds were diluted in 10% DMSO and 5 μL of the dilution was added to a 50 μL reaction so that the final concentration of DMSO was 1% in all of the reactions. All of the enzymatic reactions were conducted at 30 °C for 40 min. The 50 μL reaction mixture contained 40 mM Tris, pH 7.4, 10 mM $MgCl_2$, 0.1 mg/mL BSA, 1 mM DTT, 10 mM ATP, kinase substrate and the enzyme EGFR/VEGFR-2. After the enzymatic reaction, 50 μL of Kinase-Glo® MAX luminescence kinase assay solution was added to each reaction and the plates were incubated for 5 min at room temperature. Luminescence signal was measured using a Bio Tek Synergy 2 microplate reader (For details, please see Table S1, raw data of enzyme assay for Compounds **1** and **2** is given in the Supplementary Materials file).

2.5. In Vitro FLT-3 Inhibitory Activity

The FLT-3 assay kit (FLT-3 kinase assay, Promega Corporation, Madison, WI, USA) was designed to measure FLT-3 activity for screening and profiling applications, using ADP-Glo™ as a detection reagent. The FLT-3 kinase-glo assays were carried out in 96-well plates at 30 °C for 4 h and tested compound in a final volume of 50 μL [55,60]. Enzyme, substrate, ATP and Compounds **1** and **2** were diluted in tyrosine kinase buffer. A total 1 μL of Compounds **1** or **2** in 5% DMSO, 2 μL of enzyme (defined from Table 1), 2 μL of substrate/ATP mixture was added to the wells of 96 low volume plate and incubated at room temperature for 120 min (For details, please see Table S1. raw data of enzyme assay for Compounds **1** and **2** is given in the Supplementary Materials file).

2.6. In-Silico Binding Mechanism

Molecular docking was carried out using the Protein Data Bank (PDB) structures corresponding to the EGFR, VEGFR-2 and FLT-3 protein kinases and were downloaded from the RCSB PDB database (https://www.rcsb.org/, accessed on 5 December 2020) in PDB format. The PDB IDs used for EGFR, VEGFR-2 and FLT-3 protein kinases were 6DUK, 3VHE and 6JQR, respectively. Protein and compounds structures were energy minimized, refined and prepared for docking study by Schrödinger Maestro (Version 2018-4). OLPS3 force field and extra precision (XP) docking protocol was selected to generate induced fit

docking scores which was explained in the established procedure [5,61–66]. Van der Waals scaling factor and partial charges cutoff were selected to be 0.85 and 0.15 respectively for ligand molecules. The docking cutoff value was fixed at −10.00 kcal/mole for the screening of best poses of the docked compounds for subsequent processing.

Table 1. Inhibitory activities of Compounds **1** and **2** against MCF7 cell lines, CDK2, EGFR, VEGFR-2 and FLT-3 protein kinase.

Entry	IC_{50} (μM)	Kinase IC_{50} (μM) [a]			
	MCF7 [5]	CDK2 [5]	EGFR	VEGFR-2	FLT-3
1	1.51 ± 0.09	0.246 ± 0.05	0.269 ± 0.08	0.232 ± 0.01	1.535 ± 0.03
2	3.56 ± 0.31	0.301 ± 0.02	0.369 ± 0.32	0.266 ± 0.04	0.546 ± 0.28
Control [b–f]	3.10 ± 0.29 [b]	0.131 ± 0.24 [c]	0.056 ± 0.02 [d]	0.091 ± 0.03 [e]	0.262 ± 0.01 [f]

[a] The values are the mean ± SD of triplicate measurements; [b] Doxorubicin; [c] Imatinib; [d] Erlotinib; [e] Sorafenib; [f] Sunitinib.

3. Results

3.1. Synthesis of 1 and 2

3-((2,6-Dichlorobenzylidene)hydrazono)indolin-2-one (**1**) and 3-((2-chloro-6-fluorobenzylidene)hydrazono)indolin-2-one (**2**) were synthesized using previously reported method [5] in excellent yields.

3.2. EGFR, VEGFR-2 and FLT-3 Protein Kinase Inhibitory Activities of 1 and 2

Inhibitory activity results of Compounds **1** and **2** against EGFR, VEGFR-2 and FLT-3 protein kinases are summarized in Table 1.

As summarized in Table 1, **1** and **2** exhibited excellent inhibitory activity against EGFR, VEGFR-2 and FLT-3 comparing control drugs.

3.3. Overall Structural Arrangement of the Kinase Domain of EGFR, VEGFR-2 and FLT-3 Protein Kinases

Similar to the universal kinase domain conformations of numerous protein kinases, EGFR, VEGFR-2 and FLT-3 also exhibit a common kinase domain conformation (Figure 2) [67–69]. The main domain organization involves an *N*-terminal lobe which contains the nucleotide binding loop with its core anti-parallel *β*-sheets and a *C*-terminal lobe which comprises the activation loop and catalytic loop. The *N*- and *C*-terminal lobes are connected by a short linker. To find the conserved regions in the kinase domain of the three kinases, multiple sequence alignment was done which showed 6 highly clustered conserved residues (Figure 3).

3.4. In-Silico Binding Mechanism Analysis

Molecular docking analysis of Compound **1** with EGFR kinase domain showed several important interactions with ATP binding site residues as well as DFG motif residues, which is important for inhibition of EGFR kinase. Interactions involved hydrogen bonding interaction with ATP binding site and DFG motif residue Phe856 and π-anion interaction with Asp855 (Figure 4A,B). Binding analysis of Compound **2** with kinase domain of EGFR kinase revealed that, it formed hydrogen bond with Phe856, π-anion interaction with Asp855, π-sulfur interaction with Met790, π-alkyl interactions with Met766, Leu777, Leu747 and Leu858 (Figure 4C,D). Among them, Asp855 and Phe856 involved in the ATP binding site and DFG motif.

Docking analysis of Compound **1** with VEGFR-2 kinase domain revealed 2 hydrogen bond interactions with Cys919 and Glu917, π-π T shaped interactions with Leu840, Val848, Ala866, Lys868, Val899, Val916, Leu1035, Cys1045 and Phe1047 as well as van dar Walls interaction with Phe918 (Figure 5A,B). Compound **2** similarly made 2 hydrogen bond interactions with the gate keeper residue Cys919 and π-π T shaped interaction with DFG

motif residue Phe1047. Additionally, it formed several π-alkyl interactions as Compound **1** with the similar residues except Lys868 (Figure 5C,D).

Binding mechanism of Compound **1** with FLT-3 kinase domain involved hydrogen bond interaction with Cys694, π-π stacked binding with Tyr693, several π-alkyl interactions with Leu616, Val624, Ala642, Lys644, Val675 and Leu818. One π-sulfur interaction was observed with Cys828 (Figure 6A,B).

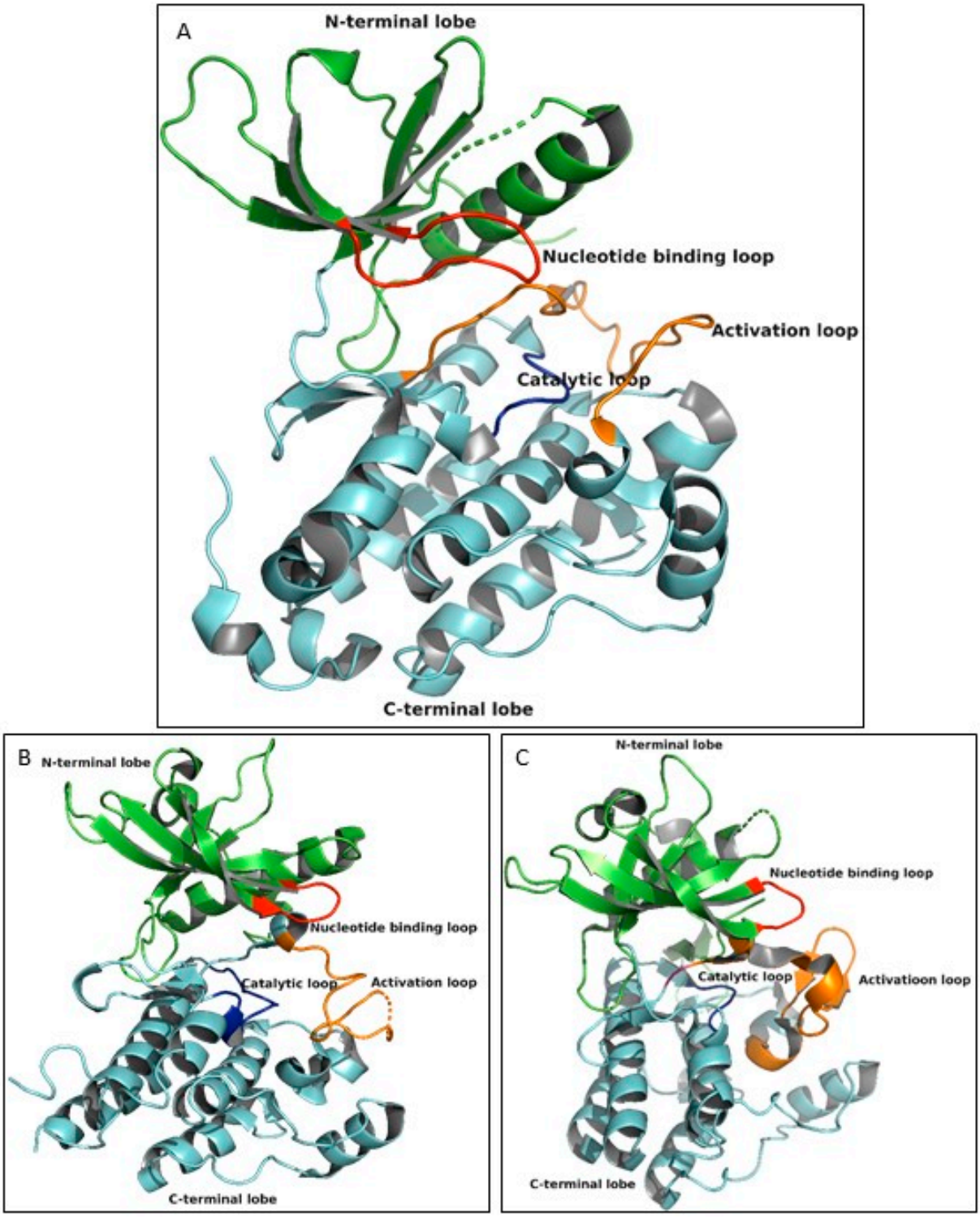

Figure 2. Overall folding of EGFR protein kinase (**A**); VEGFR-2 protein kinase (**B**) and FLT-3 protein kinase (**C**).

```
sp|P00533|EGFR_HUMAN      ---------------------------PNQALLRILKETEFKKIKVLGSGAFGTVYKGLW 33
sp|P35968|VGFR2_HUMAN     --------LPL---------DEHCERLPYDASKWEFPRDRLKLGKPLGRGAFGQVIEADA 43
sp|P36888|FLT3_HUMAN      RYESQLQMVQVTGSSDNEYFYVDFREYE-YDLKWEFPRENLEFGKVLGSGAFGKVMNATA 59
                                                        : . .::  * ** **** * :.

sp|P00533|EGFR_HUMAN      I-PEGEKVKIPVAIKELREATSPKANKEILDEAYVMASVD-NPHVCRLLGICLTS--TVQ 89
sp|P35968|VGFR2_HUMAN     FGIDKTATCRTVAVKMLKEGATHSEHRALMSELKILIHIGHHLNVVNLLGACTKPGGPLM 103
sp|P36888|FLT3_HUMAN      YGISKTGVSIQVAVKMLKEKADSSEREALMSELKMMTQLGSHENIVNLLGACTLS-GPIY 118
                             .   .   **:* *:* :  . .. ::.*  ::  :. : :: .*** *      :

sp|P00533|EGFR_HUMAN      LITQLMPFGCLLDYVREHKDN------------------------------------ 110
sp|P35968|VGFR2_HUMAN     VIVEFCKFGNLSTYLRSKRNEFVPYKTKGAR---FRQ--------GKDYVGAIPVDLKRR 152
sp|P36888|FLT3_HUMAN      LIFEYCCYGDLLNYLRSKREKFHRTWTEIFKEHNFSFYPTFQSHPNSSMPGSREVQIHPD 178
                          :* :   :* *  *:*.::::

sp|P00533|EGFR_HUMAN      ------------------------------------IGSQYLLNWCVQIAKGMNYLEDR 133
sp|P35968|VGFR2_HUMAN     LDSITSSQSSASSGFVEEKSLSDVEEEEAPEDLYKDFLTLEHLICYSFQVAKGMEFLASR 212
sp|P36888|FLT3_HUMAN      SDQISGL---HGNSFHSEDEIEYENQKRLEEEEDLNVLTFEDLLCFAYQVAKGMEFLEFK 235
                                                        :  : *: :. * **** :*  :

sp|P00533|EGFR_HUMAN      RLVHRDLAARNVLVKTPQHVKITDFGLAKLLGAEEKEYHAEGGKVPIKWMALESILHRIY 193
sp|P35968|VGFR2_HUMAN     KCIHRDLAARNILLSEKNVVKICDFGLARDIYKDPDYVRKGDARLPLKWMAPETIFDRVY 272
sp|P36888|FLT3_HUMAN      SCVHRDLAARNVLVTHGKVVKICDFGLARDIMSDSNYVVRGNARLPVKWMAPESLFEGIY 295
                             ******** *:.  : *** *****  :  : .     ..::* **** *:::. :*

sp|P00533|EGFR_HUMAN      THQSDVWSYGVTVWELMTFGSKPYDGIPASE-ISSILEKGERLPQPPICTIDVYMIMVKC 252
sp|P35968|VGFR2_HUMAN     TIQSDVWSFGVLLWEIFSLGASPYPGVKIDEEFCRRLKEGTRMRAPDYTTPEMYQTMLDC 332
sp|P36888|FLT3_HUMAN      TICSDVWSYGILLWEIFSLGVNPYPGIPVDANFYKLIQNGFKMDQPFYATEEIYIIMQSC 355
                          *  ***** *: :**::::* .** *:  .  :   :::* ::  *   * ::*  * .*

sp|P00533|EGFR_HUMAN      WMIDADSRPKFRELIIEFSKMARDPQRYLVIQGDERMHLPSPTDSNFYRA   302
sp|P35968|VGFR2_HUMAN     WHGEPSQRPTFSELVEHLGNLLQA--------------------------   356
sp|P36888|FLT3_HUMAN      WAFDSRKRPSFPNLTSFLGCQ-----------------------------   376
                          *  :  .**.* :*   :.
```

Figure 3. Multiple sequence alignment of PDB sequences from EGFR, VEGFR-2 and FLT-3 protein kinase used for docking study (red boxes implicate cluster of conserved residues where blue box represents ac-tivation loop with DFG motif). Here, asterisk "*" represents conserved residues in all three kinase domains; colon ":" shows at least two residues are conserved; and period "." indicates non-conserved residues.

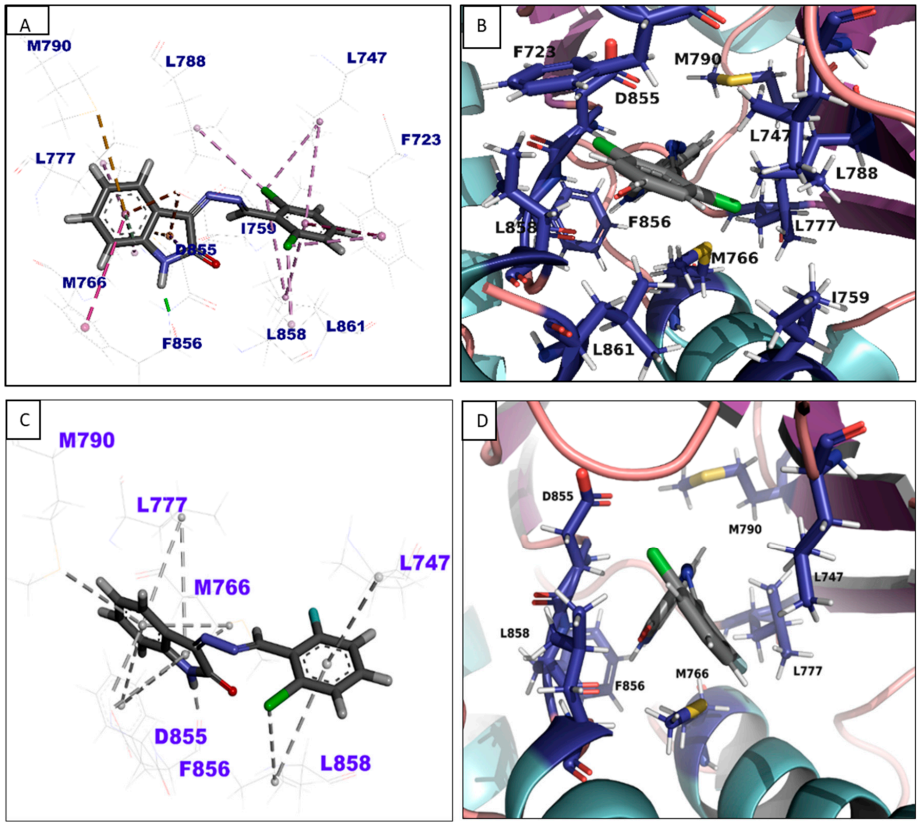

Figure 4. Docking pose of **1** and **2** within the active site of EGFR protein kinase: (**A**) 2D of **1**; (**B**) 3D of **1**; (**C**) 2D of **2**; (**D**) 3D of **2**.

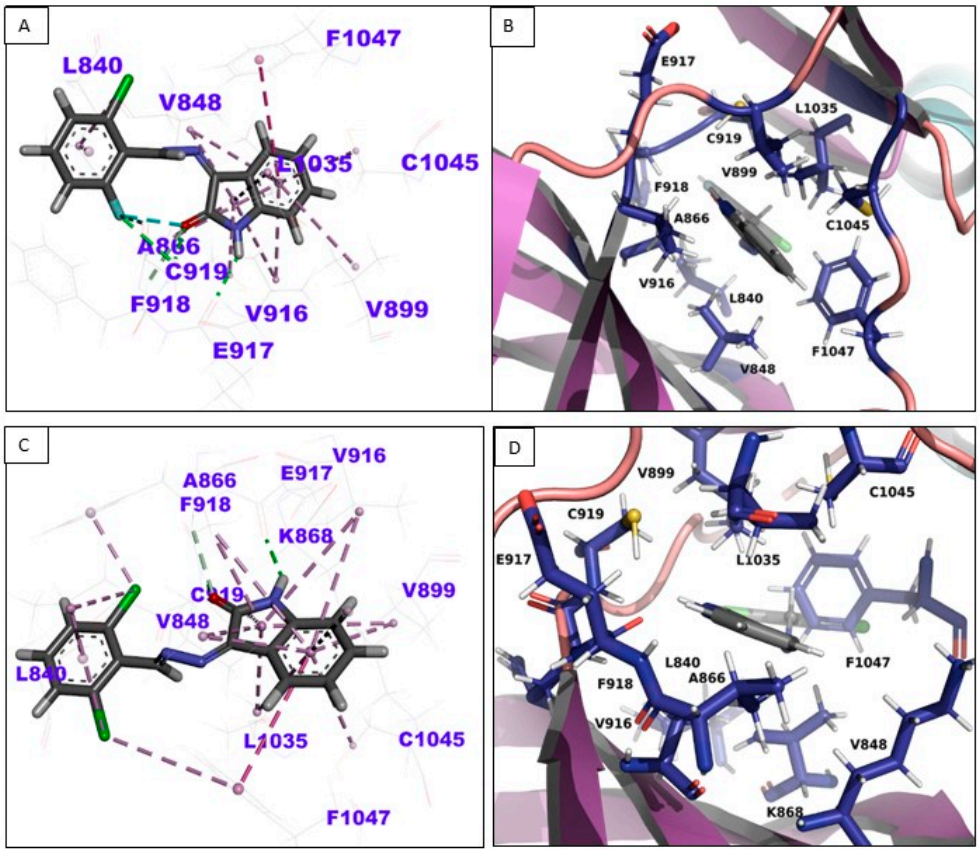

Figure 5. Docking pose of **1** and **2** within the active site of VEGFR-2 protein kinase: (**A**) 2D of **1**; (**B**) 3D of **1**; (**C**) 2D of **2**; (**D**) 3D of **2**.

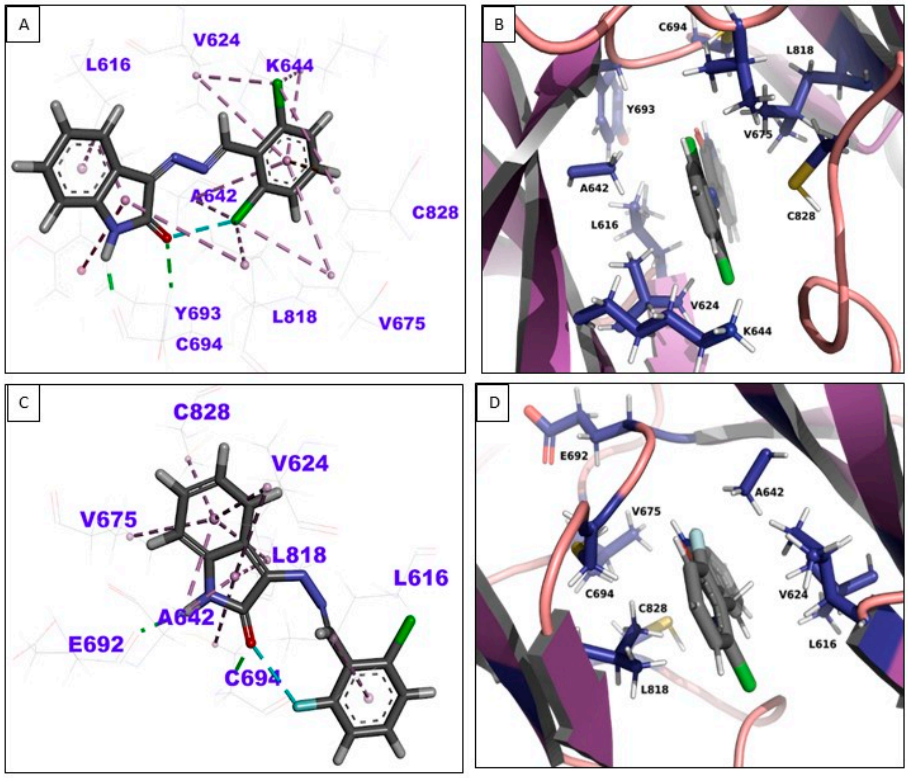

Figure 6. Docking pose of **1** and **2** within the active site of FLT-3 protein kinase: (**A**) 2D of **1**; (**B**) 3D of **1**; (**C**) 2D of **2**; (**D**) 3D of **2**.

4. Discussion

The structures of the synthesized Compounds **1** and **2** were confirmed using IR, NMR (^{1}H and ^{13}C), mass spectral data and physical properties, and compared with those reported values [5].

As reported [5], 2,6-dichloro Compound **1** exhibited excellent cytotoxicity (IC_{50} = 1.51 ± 0.09 μM (Table 1, entry 1) against human breast adenocarcinoma (MCF7) cell lines, which is two-fold more than the control anticancer drug doxorubicin (IC_{50} = 3.10 ± 0.29 μM) (Table 1, entry doxorubicin) and 2-chloro,6-fluoro substituted Compound **2** exhibited similar cytotoxicity (IC_{50} = 3.56 ± 0.31 μM) comparing to doxorubicin. In addition, both compounds were exhibited good inhibitory activity against CDK2, IC_{50} = 0.246 ± 0.05 μM and 0.301 ± 0.02 μM, respectively, which is half fold comparing to the known kinase inhibitor imatinib (IC_{50} = 0.131 ± 0.24 μM). As we know, isatin moiety containing compounds shows multiple protein kinase enzymes inhibitory activity and numbers of drugs are already in the market (Figure 1). On the other hand, both of our synthesized compounds (**1** and **2**) having isatin moiety in the structures. In addition, considering their excellent cytotoxicity as well as CDK2 inhibitory activity, we, therefore, assume that, Compounds **1** and **2** might show multiple protein kinase enzymes inhibitory activity, this led us to do further multiple protein kinase enzymes (EGFR, VEGFR-2 and FLT-3) inhibitory assay.

The IC_{50} values interpolated from dose–response data with five different concentrations were 0, 0.01, 0.1, 1 and 10 μM for all the protein kinase enzymes, EGFR, VEGFR-2 and FLT-3, respectively. Highest IC_{50} value was observed for Compound **1**, which showed IC_{50} = 1.51 ± 0.09 μM and it was twofold than the IC_{50} values of doxorubicin (3.10 ± 0.29 μM). Compound **1** also showed strong enzyme inhibitory activities against two protein kinases enzymes EGFR and VEGFR-2 with IC_{50} values of 0.269 (Figure S1) and 0.232 μM, respectively, whereas CDK2 reported [5] value showed 0.246 μM. The control drug imatinib showed 0.131 μM, erlotinib showed 0.056 μM and sorafenib showed 0.091 μM, against CDK2, EGFR, VEGFR-2 enzymes, respectively. On the other hand, Compound **2** also showed promising cytotoxicity and protein kinase inhibitory activities against all the three proteins kinase evaluated. IC_{50} value of Compound **2** was 3.56 ± 0.31 μM, which is similar to doxorubicin IC_{50} value 3.10 ± 0.29 μM [5], meanwhile its enzyme inhibitory activities against CDK2, EGFR, VEGFR-2 enzymes were 0.301, 0.369 and 0.266 μM, respectively. In case of FLT-3, Compound **1** showed 1.535 μM against FLT-3, interestingly Compound **2** showed better activity than Compound **1**, which was 0.546 μM against first FLT-3 inhibitor sunitinib (sunitinib was 0.262 μM), which prolonged haemotoxicity and hand-foot syndrome caused by FLT-3 mutated acute myeloid leukaemia (AML) [70].

In our previous study [5] we have reported that, Compounds **1** and **2** inhibited CDK2 kinase in an ATP dependent manner and acted as type II inhibitor by lacking DFG motif interaction in the activation loop. Interaction with DFG motif residues is crucial for an inhibitor to define as active or inactive state kinase inhibition. Similarly, in this experiment, the interaction of Compounds **1** and **2** with EGFR, VEGFR-2 and FLT-3 protein kinases was evaluated by molecular docking analysis.

Since Compound **1** with EGFR kinase domain showed several important interactions and involved hydrogen bonding interactions with ATP binding site and DFG motif residue, thus, it can be said that, Compound **1** might act on active kinase by interacting with DFG motif residues. It also formed several π-π stacked and π-π T shaped interactions with Met766, Met790, Phe723, Leu747, Leu777, Leu788, Ile759, Leu858 and Leu861. Compound **2** with kinase domain of EGFR kinase formed hydrogen bond. Among the hydrogen bonds, Asp855 and Phe856 involved in the ATP binding site and DFG motif, thus, Compound **2** can act as type I inhibitor by active against EGFR kinase. The interactions of both compounds (**1** and **2**) with EGFR kinase showed ATP competitive inhibition and thus support previous experiments [71,72]. Compound **1** with VEGFR-2 kinase domain revealed two hydrogen bond interactions with Cys919 and Glu917, π-π T shaped interactions with many residues, as well as van dar Walls interaction, therefore, it was clear from the analysis that, Compound

1 can interact with the DFG motif residue Phe1047 of the ATP binding site Cys919 of the hinge region which also act as a gate keeper residue. Compound **2** similarly made two hydrogen bond interactions with the gate keeper residue, and additionally, it formed several π-alkyl interactions as Compound **1** with the similar residues except Lys868. The interactions of Compounds **1** and **2** with the kinase domain is consistent with the previous docking results which showed similar interaction of the synthesized compounds [73,74]. Therefore, the docking result of Compounds **1** and **2** with the kinase domain of VEGFR-2 showed similar fashion of interactions involving both DFG motif and hinge region (which comprise the ATP binding site) interaction could possibly make them type I ATP competitive inhibitor (DFG motif interaction implies active state of kinase) against VEGFR-2 kinase. The interactions of Compound 1 and Flt-3 kinase domain involve hydrogen bond. Previously published co-crystal structure of FLT-3 with Quizartinib showed that, interactions with Phe830 in the DFG motif and Phe691 in the hinge region would be crucial for inhibition of the active kinase [75]. However, Compound **1** lacked these interactions. The interactions between Compound 2 and Flt-3 kinase domain lack active state kinase residues. However, it showed several hydrogen and ionic bond interactions similar to Compound **1** except Glu692. It lacked interaction with Tyr693 compared to Compound **1**. Finally, from the docking result of Compounds **1** and **2** with FLT-3 kinase domain it can be concluded that both compounds lacked active state kinase domain interactions and lacked interactions with hinge region of the ATP binding site and can be considered as type II inhibitor in case of FLT-3 kinase but not as ATP competitive inhibitor.

5. Conclusions

In conclusion, isatin hydrazones **1** and **2** exhibited excellent inhibitory activity against EGFR, VEGFR-2 and FLT-3 protein kinases. Binding mechanism analysis by molecular docking study of **1** and **2** revealed that, both compounds acted as type I ATP competitive inhibitor against EGFR and VEGFR-2 kinase by interacting with DFG motif and hinge region of ATP binding site. However, they lacked important interactions with ATP binding site residues of FLT-3 kinase thus might act as type II ATP non-competitive inhibitor.

Supplementary Materials: The following are available online at https://www.mdpi.com/article/10.3390/app11093746/s1, Figure S1: Calculation of the IC_{50} Values of Protein Kinase Enzyme EGFR for Compound **1**, Table S1: Enzyme assays for Compounds **1** and **2** and Experimental Data for Compounds **1** and **2**.

Author Contributions: Conceptualization, H.S.A.-S. and A.F.M.M.R.; methodology, I.S.I. and M.A.; software, M.A.; validation, A.F.M.M.R. and H.S.A.-S.; formal analysis, I.S.I. and M.A.; investigation, H.S.A.-S. and A.F.M.M.R.; resources, H.S.A.-S.; data curation, M.A. and I.S.I.; writing—original draft preparation, A.F.M.M.R.; writing—review and editing, A.F.M.M.R. and H.S.A.-S.; visualization, M.A.; supervision, A.F.M.M.R. and H.S.A.-S.; project administration, H.S.A.-S.; funding acquisition, H.S.A.-S. All authors have read and agreed to the published version of the manuscript.

Funding: This research was funded by the King Saud University, Research Center of the Female Campus for Scientific and Medical Studies.

Institutional Review Board Statement: Not applicable.

Informed Consent Statement: Not applicable.

Data Availability Statement: Not applicable.

Acknowledgments: This research project was supported by a grant from the research center of the Female Campus for Scientific and Medical Studies, King Saud University, Riyadh, Saudi Arabia.

Conflicts of Interest: The authors declare no conflict of interest.

References

1. Kozlov, S.; Waters, N.C.; Chavchich, M. Leveraging cell cycle analysis in anticancer drug discovery to identify novel plasmodial drug targets. *Infect. Disord. Drug Targets* **2010**, *10*, 165–190. [CrossRef] [PubMed]
2. Rahman, A.F.M.M.; Park, S.-E.; Kadi, A.A.; Kwon, Y. Fluorescein Hydrazones as Novel Nonintercalative Topoisomerase Catalytic Inhibitors with Low DNA Toxicity. *J. Med. Chem.* **2014**, *57*, 9139–9151. [CrossRef] [PubMed]
3. Ahmad, P.; Woo, H.; Jun, K.-Y.; Kadi, A.A.; Abdel-Aziz, H.A.; Kwon, Y.; Rahman, A.F.M.M. Design, synthesis, topoisomerase I & II inhibitory activity, antiproliferative activity, and structure–activity relationship study of pyrazoline derivatives: An ATP-competitive human topoisomerase IIα catalytic inhibitor. *Bioorg. Med. Chem.* **2016**, *24*, 1898–1908. [CrossRef]
4. Islam, M.S.; Park, S.; Song, C.; Kadi, A.A.; Kwon, Y.; Rahman, A.F.M.M. Fluorescein hydrazones: A series of novel non-intercalative topoisomerase IIα catalytic inhibitors induce G1 arrest and apoptosis in breast and colon cancer cells. *Eur. J. Med. Chem.* **2017**, *125*, 49–67. [CrossRef] [PubMed]
5. Al-Salem, H.S.; Arifuzzaman, M.; Alkahtani, H.M.; Abdalla, A.N.; Issa, I.S.; Alqathama, A.; Albalawi, F.S.; Rahman, A.F.M.M. A Series of Isatin-Hydrazones with Cytotoxic Activity and CDK2 Kinase Inhibitory Activity: A Potential Type II ATP Competitive Inhibitor. *Molecules* **2020**, *25*, 4400. [CrossRef] [PubMed]
6. Herbst, R.S. Review of epidermal growth factor receptor biology. *Int. J. Radiat. Oncol. Biol. Phys.* **2004**, *59*, 21–26. [CrossRef]
7. Zhang, X.; Mar, V.; Zhou, W.; Harrington, L.; Robinson, M.O. Telomere shortening and apoptosis in telomerase-inhibited human tumor cells. *Genes Dev.* **1999**, *13*, 2388–2399. [CrossRef]
8. Bishayee, S. Role of conformational alteration in the epidermal growth factor receptor (EGFR) function. *Biochem. Pharmacol.* **2000**, *60*, 1217–1223. [CrossRef]
9. Umekita, Y.; Ohi, Y.; Sagara, Y.; Yoshida, H. Co-expression of epidermal growth factor receptor and transforming growth factor-alpha predicts worse prognosis in breast-cancer patients. *Int. J. Cancer* **2000**, *89*, 484–487. [CrossRef]
10. Ogiso, H.; Ishitani, R.; Nureki, O.; Fukai, S.; Yamanaka, M.; Kim, J.H.; Saito, K.; Sakamoto, A.; Inoue, M.; Shirouzu, M.; et al. Crystal structure of the complex of human epidermal growth factor and receptor extracellular domains. *Cell* **2002**, *110*, 775–787. [CrossRef]
11. Hirsch, F.R.; Varella-Garcia, M.; Bunn, P.A., Jr.; Di Maria, M.V.; Veve, R.; Bremmes, R.M.; Barón, A.E.; Zeng, C.; Franklin, W.A. Epidermal growth factor receptor in non-small-cell lung carcinomas: Correlation between gene copy number and protein expression and impact on prognosis. *J. Clin. Oncol.* **2003**, *21*, 3798–3807. [CrossRef]
12. Bazley, L.A.; Gullick, W.J. The epidermal growth factor receptor family. *Endocr.-Relat. Cancer* **2005**, *12*, S17–S27. [CrossRef] [PubMed]
13. Zhang, H.; Berezov, A.; Wang, Q.; Zhang, G.; Drebin, J.; Murali, R.; Greene, M.I. ErbB receptors: From oncogenes to targeted cancer therapies. *J. Clin. Investig.* **2007**, *117*, 2051–2058. [CrossRef]
14. Ivanković, M.; Cukusić, A.; Gotić, I.; Skrobot, N.; Matijasić, M.; Polancec, D.; Rubelj, I. Telomerase activity in HeLa cervical carcinoma cell line proliferation. *Biogerontology* **2007**, *8*, 163–172. [CrossRef] [PubMed]
15. Wei, G.; Cui, S.; Luan, W.; Wang, S.; Hou, Z.; Liu, Y.; Cheng, M. Natural product-based design, synthesis and biological evaluation of Albiziabioside A derivatives that selectively induce HCT116 cell death. *Eur. J. Med. Chem.* **2016**, *113*, 92–101. [CrossRef] [PubMed]
16. Holmes, K.; Roberts, O.L.; Thomas, A.M.; Cross, M.J. Vascular endothelial growth factor receptor-2: Structure, function, intracellular signalling and therapeutic inhibition. *Cell Signal.* **2007**, *19*, 2003–2012. [CrossRef]
17. Stuttfeld, E.; Ballmer-Hofer, K. Structure and function of VEGF receptors. *IUBMB Life* **2009**, *61*, 915–922. [CrossRef]
18. Lu, R.-M.; Chiu, C.-Y.; Liu, I.-J.; Chang, Y.-L.; Liu, Y.-J.; Wu, H.-C. Novel human Ab against vascular endothelial growth factor receptor 2 shows therapeutic potential for leukemia and prostate cancer. *Cancer Sci.* **2019**, *110*, 3773–3787. [CrossRef]
19. Rosnet, O.; Matteï, M.G.; Marchetto, S.; Birnbaum, D. Isolation and chromosomal localization of a novel FMS-like tyrosine kinase gene. *Genomics* **1991**, *9*, 380–385. [CrossRef]
20. Rosnet, O.; Schiff, C.; Pébusque, M.J.; Marchetto, S.; Tonnelle, C.; Toiron, Y.; Birg, F.; Birnbaum, D. Human FLT3/FLK2 gene: cDNA cloning and expression in hematopoietic cells. *Blood* **1993**, *82*, 1110–1119. [CrossRef]
21. Lemmon, M.A.; Schlessinger, J. Cell Signaling by Receptor Tyrosine Kinases. *Cell* **2010**, *141*, 1117–1134. [CrossRef]
22. Birg, F.; Courcoul, M.; Rosnet, O.; Bardin, F.; Pébusque, M.J.; Marchetto, S.; Tabilio, A.; Mannoni, P.; Birnbaum, D. Expression of the FMS/KIT-like gene FLT3 in human acute leukemias of the myeloid and lymphoid lineages. *Blood* **1992**, *80*, 2584–2593. [CrossRef]
23. Hannum, C.; Culpepper, J.; Campbell, D.; McClanahan, T.; Zurawski, S.; Bazan, J.F.; Kastelein, R.; Hudak, S.; Wagner, J.; Mattson, J.; et al. Ligand for FLT3/FLK2 receptor tyrosine kinase regulates growth of haematopoietic stem cells and is encoded by variant RNAs. *Nature* **1994**, *368*, 643–648. [CrossRef]
24. Kiyoi, H.; Naoe, T.; Nakano, Y.; Yokota, S.; Minami, S.; Miyawaki, S.; Asou, N.; Kuriyama, K.; Jinnai, I.; Shimazaki, C.; et al. Prognostic implication of FLT3 and N-RAS gene mutations in acute myeloid leukemia. *Blood* **1999**, *93*, 3074–3080. [CrossRef] [PubMed]
25. Kiyoi, H.; Kawashima, N.; Ishikawa, Y. FLT3 mutations in acute myeloid leukemia: Therapeutic paradigm beyond inhibitor development. *Cancer Sci.* **2020**, *111*, 312–322. [CrossRef]
26. El-Husseiny, W.M.; El-Sayed, M.A.A.; Abdel-Aziz, N.I.; El-Azab, A.S.; Ahmed, E.R.; Abdel-Aziz, A.A.M. Synthesis, antitumour and antioxidant activities of novel α,β-unsaturated ketones and related heterocyclic analogues: EGFR inhibition and molecular modelling study. *J. Enzym. Inhib. Med. Chem.* **2018**, *33*, 507–518. [CrossRef]

27. Miura, M. Therapeutic drug monitoring of imatinib, nilotinib, and dasatinib for patients with chronic myeloid leukemia. *Biol. Pharm. Bull.* **2015**, *38*, 645–654. [CrossRef] [PubMed]
28. Stamos, J.; Sliwkowski, M.X.; Eigenbrot, C. Structure of the epidermal growth factor receptor kinase domain alone and in complex with a 4-anilinoquinazoline inhibitor. *J. Biol. Chem.* **2002**, *277*, 46265–46272. [CrossRef]
29. Rabindran, S.K.; Discafani, C.M.; Rosfjord, E.C.; Baxter, M.; Floyd, M.B.; Golas, J.; Hallett, W.A.; Johnson, B.D.; Nilakantan, R.; Overbeek, E.; et al. Antitumor activity of HKI-272, an orally active, irreversible inhibitor of the HER-2 tyrosine kinase. *Cancer Res.* **2004**, *64*, 3958–3965. [CrossRef]
30. Minami, Y.; Shimamura, T.; Shah, K.; LaFramboise, T.; Glatt, K.A.; Liniker, E.; Borgman, C.L.; Haringsma, H.J.; Feng, W.; Weir, B.A.; et al. The major lung cancer-derived mutants of ERBB2 are oncogenic and are associated with sensitivity to the irreversible EGFR/ERBB2 inhibitor HKI-272. *Oncogene* **2007**, *26*, 5023–5027. [CrossRef] [PubMed]
31. Wissner, A.; Mansour, T.S. The development of HKI-272 and related compounds for the treatment of cancer. *Arch. Pharm.* **2008**, *341*, 465–477. [CrossRef]
32. Morgillo, F.; Martinelli, E.; Troiani, T.; Orditura, M.; De Vita, F.; Ciardiello, F. Antitumor activity of sorafenib in human cancer cell lines with acquired resistance to EGFR and VEGFR tyrosine kinase inhibitors. *PLoS ONE* **2011**, *6*, e28841. [CrossRef] [PubMed]
33. Ou, S.H. Crizotinib: A novel and first-in-class multitargeted tyrosine kinase inhibitor for the treatment of anaplastic lymphoma kinase rearranged non-small cell lung cancer and beyond. *Drug Des. Dev. Ther.* **2011**, *5*, 471–485. [CrossRef]
34. Yasuda, H.; de Figueiredo-Pontes, L.L.; Kobayashi, S.; Costa, D.B. Preclinical rationale for use of the clinically available multitargeted tyrosine kinase inhibitor crizotinib in ROS1-translocated lung cancer. *J. Thorac. Oncol.* **2012**, *7*, 1086–1090. [CrossRef] [PubMed]
35. Yamaguchi, N.; Lucena-Araujo, A.R.; Nakayama, S.; de Figueiredo-Pontes, L.L.; Gonzalez, D.A.; Yasuda, H.; Kobayashi, S.; Costa, D.B. Dual ALK and EGFR inhibition targets a mechanism of acquired resistance to the tyrosine kinase inhibitor crizotinib in ALK rearranged lung cancer. *Lung Cancer* **2014**, *83*, 37–43. [CrossRef]
36. Lee, J.Y.; Lee, Y.M.; Chang, G.C.; Yu, S.L.; Hsieh, W.Y.; Chen, J.J.; Chen, H.W.; Yang, P.C. Curcumin induces EGFR degradation in lung adenocarcinoma and modulates p38 activation in intestine: The versatile adjuvant for gefitinib therapy. *PLoS ONE* **2011**, *6*, e23756. [CrossRef]
37. Lv, P.C.; Li, D.D.; Li, Q.S.; Lu, X.; Xiao, Z.P.; Zhu, H.L. Synthesis, molecular docking and evaluation of thiazolyl-pyrazoline derivatives as EGFR TK inhibitors and potential anticancer agents. *Bioorg. Med. Chem. Lett.* **2011**, *21*, 5374–5377. [CrossRef] [PubMed]
38. Xu, Y.Y.; Cao, Y.; Ma, H.; Li, H.Q.; Ao, G.Z. Design, synthesis and molecular docking of α,β-unsaturated cyclohexanone analogous of curcumin as potent EGFR inhibitors with antiproliferative activity. *Bioorg. Med. Chem.* **2013**, *21*, 388–394. [CrossRef] [PubMed]
39. Jung, S.K.; Lee, M.H.; Lim, D.Y.; Kim, J.E.; Singh, P.; Lee, S.Y.; Jeong, C.H.; Lim, T.G.; Chen, H.; Chi, Y.I.; et al. Isoliquiritigenin induces apoptosis and inhibits xenograft tumor growth of human lung cancer cells by targeting both wild type and L858R/T790M mutant EGFR. *J. Biol. Chem.* **2014**, *289*, 35839–35848. [CrossRef]
40. Wada, K.; Lee, J.Y.; Hung, H.Y.; Shi, Q.; Lin, L.; Zhao, Y.; Goto, M.; Yang, P.C.; Kuo, S.C.; Chen, H.W.; et al. Novel curcumin analogs to overcome EGFR-TKI lung adenocarcinoma drug resistance and reduce EGFR-TKI-induced GI adverse effects. *Bioorg. Med. Chem.* **2015**, *23*, 1507–1514. [CrossRef]
41. Alswah, M.; Bayoumi, A.H.; Elgamal, K.; Elmorsy, A.; Ihmaid, S.; Ahmed, H.E.A. Design, Synthesis and Cytotoxic Evaluation of Novel Chalcone Derivatives Bearing Triazolo [4, 3-a]-quinoxaline Moieties as Potent Anticancer Agents with Dual EGFR Kinase and Tubulin Polymerization Inhibitory Effects. *Molecules* **2017**, *23*, 48. [CrossRef]
42. Whittles, C.E.; Pocock, T.M.; Wedge, S.R.; Kendrew, J.; Hennequin, L.F.; Harper, S.J.; Bates, D.O. ZM323881, a Novel Inhibitor of Vascular Endothelial Growth Factor-Receptor-2 Tyrosine Kinase Activity. *Microcirculation* **2002**, *9*, 513–522. [CrossRef]
43. Jost, L.; Gschwind, H.-P.; Jalava, T.; Wang, Y.; Guenther, C.; Souppart, C.; Rottmann, A.; Denner, K.; Waldmeier, F.; Gross, G.; et al. Metabolism and Disposition of Vatalanib (PTK787/ZK-222584) in Cancer Patients. *Drug Metab. Dispos.* **2006**, *34*, 1817–1828. [CrossRef] [PubMed]
44. Harmange, J.-C.; Weiss, M.M.; Germain, J.; Polverino, A.J.; Borg, G.; Bready, J.; Chen, D.; Choquette, D.; Coxon, A.; DeMelfi, T.; et al. Naphthamides as Novel and Potent Vascular Endothelial Growth Factor Receptor Tyrosine Kinase Inhibitors: Design, Synthesis, and Evaluation. *J. Med. Chem.* **2008**, *51*, 1649–1667. [CrossRef] [PubMed]
45. Nikolinakos, P.; Heymach, J.V. The tyrosine kinase inhibitor cediranib for non-small cell lung cancer and other thoracic malignancies. *J. Thorac. Oncol.* **2008**, *3*, S131–S134. [CrossRef]
46. Kubota, K.; Ichinose, Y.; Scagliotti, G.; Spigel, D.; Kim, J.H.; Shinkai, T.; Takeda, K.; Kim, S.W.; Hsia, T.C.; Li, R.K.; et al. Phase III study (MONET1) of motesanib plus carboplatin/paclitaxel in patients with advanced nonsquamous nonsmall-cell lung cancer (NSCLC): Asian subgroup analysis. *Ann. Oncol.* **2014**, *25*, 529–536. [CrossRef] [PubMed]
47. Soria, J.C.; DeBraud, F.; Bahleda, R.; Adamo, B.; Andre, F.; Dientsmann, R.; Delmonte, A.; Cereda, R.; Isaacson, J.; Litten, J.; et al. Phase I/IIa study evaluating the safety, efficacy, pharmacokinetics, and pharmacodynamics of lucitanib in advanced solid tumors. *Ann. Oncol.* **2014**, *25*, 2244–2251. [CrossRef]
48. Guffanti, F.; Chilà, R.; Bello, E.; Zucchetti, M.; Zangarini, M.; Ceriani, L.; Ferrari, M.; Lupi, M.; Jacquet-Bescond, A.; Burbridge, M.F.; et al. In Vitro and In Vivo Activity of Lucitanib in FGFR1/2 Amplified or Mutated Cancer Models. *Neoplasia* **2017**, *19*, 35–42. [CrossRef] [PubMed]

49. Peng, F.-W.; Liu, D.-K.; Zhang, Q.-W.; Xu, Y.-G.; Shi, L. VEGFR-2 inhibitors and the therapeutic applications thereof: A patent review (2012-2016). *Expert Opin. Ther. Pat.* **2017**, *27*, 987–1004. [CrossRef] [PubMed]
50. Modi, S.J.; Kulkarni, V.M. Vascular Endothelial Growth Factor Receptor (VEGFR-2)/KDR Inhibitors: Medicinal Chemistry Perspective. *Med. Drug Discov.* **2019**, *2*, 100009. [CrossRef]
51. Chung, T.-W.; Kim, E.-Y.; Choi, H.-J.; Han, C.W.; Jang, S.B.; Kim, K.-J.; Jin, L.; Koh, Y.J.; Ha, K.-T. 6′-Sialylgalactose inhibits vascular endothelial growth factor receptor 2-mediated angiogenesis. *Exp. Mol. Med.* **2019**, *51*, 1–13. [CrossRef]
52. Wu, M.; Li, C.; Zhu, X. FLT3 inhibitors in acute myeloid leukemia. *J. Hematol. Oncol.* **2018**, *11*, 133. [CrossRef] [PubMed]
53. Short, N.J.; Kantarjian, H.; Ravandi, F.; Daver, N. Emerging treatment paradigms with FLT3 inhibitors in acute myeloid leukemia. *Ther. Adv. Hematol.* **2019**, *10*, 204062071982731. [CrossRef] [PubMed]
54. Zhao, J.; Song, Y.; Liu, D. Gilteritinib: A novel FLT3 inhibitor for acute myeloid leukemia. *Biomark. Res.* **2019**, *7*, 19. [CrossRef] [PubMed]
55. Antar, A.I.; Otrock, Z.K.; Jabbour, E.; Mohty, M.; Bazarbachi, A. FLT3 inhibitors in acute myeloid leukemia: Ten frequently asked questions. *Leukemia* **2020**, *34*, 682–696. [CrossRef] [PubMed]
56. Tong, L.; Li, X.; Hu, Y.; Liu, T. Recent advances in FLT3 inhibitors for acute myeloid leukemia. *Future Med. Chem.* **2020**, *12*, 961–981. [CrossRef] [PubMed]
57. Tarver, T.C.; Hill, J.E.; Rahmat, L.; Perl, A.E.; Bahceci, E.; Mori, K.; Smith, C.C. Gilteritinib is a clinically active FLT3 inhibitor with broad activity against FLT3 kinase domain mutations. *Blood Adv.* **2020**, *4*, 514–524. [CrossRef] [PubMed]
58. Manetti, F.; Locatelli, G.A.; Maga, G.; Schenone, S.; Modugno, M.; Forli, S.; Corelli, F.; Botta, M. A Combination of Docking/Dynamics Simulations and Pharmacophoric Modeling to Discover New Dual c-Src/Abl Kinase Inhibitors. *J. Med. Chem.* **2006**, *49*, 3278–3286. [CrossRef]
59. Abbas, H.-A.S.; Abd El-Karim, S.S. Design, synthesis and anticervical cancer activity of new benzofuran–pyrazol-hydrazono-thiazolidin-4-one hybrids as potential EGFR inhibitors and apoptosis inducing agents. *Bioorg. Chem.* **2019**, *89*, 103035. [CrossRef]
60. Larrosa-Garcia, M.; Baer, M.R. FLT3 Inhibitors in Acute Myeloid Leukemia: Current Status and Future Directions. *Mol. Cancer Ther.* **2017**, *16*, 991–1001. [CrossRef]
61. Pradeepkiran, J.A.; Kumar, K.K.; Kumar, Y.N.; Bhaskar, M. Modeling, molecular dynamics, and docking assessment of transcription factor rho: A potential drug target in *Brucella melitensis* 16M. *Drug Des. Dev. Ther.* **2015**, *9*, 1897–1912. [CrossRef]
62. Pradeepkiran, J.A.; Sainath, S.B.; Kumar, K.K.; Bhaskar, M. Complete genome-wide screening and subtractive genomic approach revealed new virulence factors, potential drug targets against bio-war pathogen *Brucella melitensis* 16M. *Drug Des. Dev. Ther.* **2015**, *9*, 1691–1706. [CrossRef]
63. Sudhana, S.M.; Adi, P.J. Synthesis, Biological Evaluation and Molecular Docking Studies of Novel Di-hydropyridine Analogs as Potent Antioxidants. *Curr. Top. Med. Chem.* **2019**, *19*, 2676–2686. [CrossRef]
64. Pradeepkiran, J.A.; Reddy, P.H. Structure Based Design and Molecular Docking Studies for Phosphorylated Tau Inhibitors in Alzheimer's Disease. *Cells* **2019**, *8*, 260. [CrossRef]
65. Pradeepkiran, J.A.; Reddy, A.P.; Reddy, P.H. Pharmacophore-based models for therapeutic drugs against phosphorylated tau in Alzheimer's disease. *Drug Discov. Today* **2019**, *24*, 616–623. [CrossRef]
66. Pradeepkiran, J.A.; Reddy, A.P.; Yin, X.; Manczak, M.; Reddy, P.H. Protective effects of BACE1 inhibitory ligand molecules against amyloid beta-induced synaptic and mitochondrial toxicities in Alzheimer's disease. *Hum. Mol. Genet.* **2020**, *29*, 49–69. [CrossRef] [PubMed]
67. McTigue, M.A.; Wickersham, J.A.; Pinko, C.; Showalter, R.E.; Parast, C.V.; Tempczyk-Russell, A.; Gehring, M.R.; Mroczkowski, B.; Kan, C.C.; Villafranca, J.E.; et al. Crystal structure of the kinase domain of human vascular endothelial growth factor receptor 2: A key enzyme in angiogenesis. *Structure* **1999**, *7*, 319–330. [CrossRef]
68. Griffith, J.; Black, J.; Faerman, C.; Swenson, L.; Wynn, M.; Lu, F.; Lippke, J.; Saxena, K. The structural basis for autoinhibition of FLT3 by the juxtamembrane domain. *Mol. Cell* **2004**, *13*, 169–178. [CrossRef]
69. Zhang, X.; Gureasko, J.; Shen, K.; Cole, P.A.; Kuriyan, J. An allosteric mechanism for activation of the kinase domain of epidermal growth factor receptor. *Cell* **2006**, *125*, 1137–1149. [CrossRef]
70. Fiedler, W.; Kayser, S.; Kebenko, M.; Janning, M.; Krauter, J.; Schittenhelm, M.; Götze, K.; Weber, D.; Göhring, G.; Teleanu, V.; et al. A phase I/II study of sunitinib and intensive chemotherapy in patients over 60 years of age with acute myeloid leukaemia and activating FLT3 mutations. *Br. J. Haematol.* **2015**, *169*, 694–700. [CrossRef]
71. Liao, Q.H.; Gao, Q.Z.; Wei, J.; Chou, K.C. Docking and molecular dynamics study on the inhibitory activity of novel inhibitors on epidermal growth factor receptor (EGFR). *Med. Chem.* **2011**, *7*, 24–31. [CrossRef] [PubMed]
72. Belal, A. Synthesis, molecular docking and antitumor activity of novel pyrrolizines with potential as EGFR-TK inhibitors. *Bioorg. Chem.* **2015**, *59*, 124–129. [CrossRef] [PubMed]
73. Kunz, R.K.; Rumfelt, S.; Chen, N.; Zhang, D.; Tasker, A.S.; Bürli, R.; Hungate, R.; Yu, V.; Nguyen, Y.; Whittington, D.A.; et al. Discovery of amido-benzisoxazoles as potent c-Kit inhibitors. *Bioorg. Med. Chem. Lett.* **2008**, *18*, 5115–5117. [CrossRef] [PubMed]
74. Aziz, M.A.; Serya, R.A.T.; Lasheen, D.S.; Abdel-Aziz, A.K.; Esmat, A.; Mansour, A.M.; Singab, A.N.B.; Abouzid, K.A.M. Discovery of Potent VEGFR-2 Inhibitors based on Furopyrimidine and Thienopyrimidne Scaffolds as Cancer Targeting Agents. *Sci. Rep.* **2016**, *6*, 24460. [CrossRef]
75. Zorn, J.A.; Wang, Q.; Fujimura, E.; Barros, T.; Kuriyan, J. Crystal Structure of the FLT3 Kinase Domain Bound to the Inhibitor Quizartinib (AC220). *PLoS ONE* **2015**, *10*, e0121177. [CrossRef] [PubMed]